Model-Based Estimation of Heating Element Temperature Using Resistance Measurement

Suhail S. Saquib and Brian Busch, Polaroid Corporation, Waltham, Massachusetts, USA

Abstract

The resistance of a thermal print head's heating element typically changes with temperature. This property is exploited to estimate the temperature of the element. The proposed method employs a model for the temperature rise when power is applied to the element in conjunction with a model for mapping the resistance to temperature. The parameters of the model are learned from the resistance measurements using a maximum likelihood estimator. An analytical expression is obtained for the bias in the estimated parameters. Results for synthetic and real data show that the proposed methods estimate the resistance-temperature mapping with a high degree of accuracy.

Introduction

The resistivity of the material chosen for fabricating the heating elements of a thermal print head typically exhibits some temperature dependence. This property has been utilized in the past by the NEC/Susumu thermal print head (TPH) for actively controlling the heating element to maintain a desired temperature.[1] Other potential applications include the compensation of TPH-to-TPH variability, and the estimation of the thermal model parameters for improved thermal history control.[2]

All of these applications require the resistance-temperature mapping of the heating element in its operating temperature range, which is much higher than the maximum allowable heat-sink temperature. We propose to estimate this mapping from resistance measurements made over a limited range of heat-sink temperatures of the TPH. The method employs a model for predicting the element's temperature as a function of applied power in conjunction with a model for the resistance-temperature mapping. This model-based approach is capable of learning the functional relationship between the element's resistance and its temperature for temperatures much higher than the maximum allowable heat-sink temperature. A maximum likelihood estimator (MLE) is proposed to learn the model parameters from the measurements. We show that the MLE for jointly estimating the temperature model and resistance-temperature mapping is biased. We derive an analytical expression for this bias and identify the factors that contribute to it.

Experimental Apparatus

The resistance measurement apparatus is shown in Fig. 1.

This is a classical "bridge" configuration. The resistors R_1 and R_2 are chosen to be small to minimize any RC time-constant delays in the measurement system, and the resistor R_b is chosen to approximately match the TPH resistance. When current is provided to an element of the TPH, the currents in the two arms of the bridge are nearly equal, and the voltage sampled by the op-amp is nearly zero. Batteries supply all electrical power to the circuit in order to minimize noise, and all supply voltages are regulated (not shown).

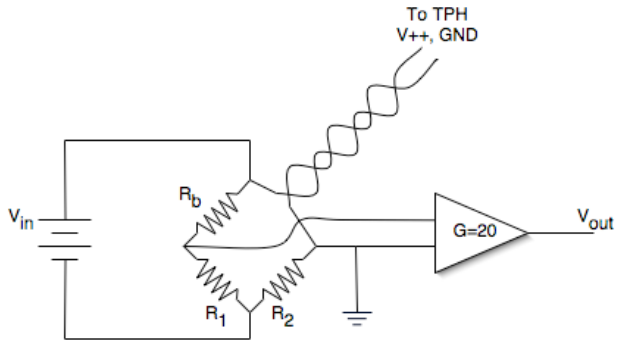

Figure 1. The above figure shows a schematic of the resistance measurement apparatus

The op-amp is chosen to have a high gain-bandwidth product and low noise, to allow for high-speed measurements of the instantaneous resistance. The op-amp's gain (G) and input offset (V_{off}), as well as the values of R_1 and R_2 are carefully calibrated using fixed, precision resistors in place of the TPH. To eliminate the effects of temperature drift on the resistors and the op-amp, the entire circuit board is kept in an insulated box maintained at a constant temperature .

The output of the op-amp (V_{out}) and the input voltage (V_{in}) are recorded on a digitizing oscilloscope for analysis. The instantaneous resistance is computed as

$$R \quad \frac{GR_2R_bV_{in} \quad R_2 \; R_1 \quad R_b \quad V_{out} \quad GV_{off}}{GR_1V_{in} \quad R_1 \quad R_b \quad V_{out} \quad GV_{off}} \tag{1}$$

The TPH is placed in an oven and is allowed to come to thermal equilibrium before any measurements are made. This allows for accurate measurement of the initial temperature of the heating elements before application of power. Resistance measurements are made for a variety of initial heat-sink temperatures of the TPH after applying power for a fixed duration of time ("on-time").

Heating Element Temperature Estimation

Let $T = f(R)$ denote the unknown function that maps the resistance of the heating element R to its temperature T. The function $f(\cdot)$ is a

characteristic of the material used to construct the heating elements. We are interested in estimating $f(\cdot)$ from the resistance measurements. In the process of measuring the resistance, some current has to be supplied to the heating element raising its temperature. Consequently, the temperature at which the resistance measurement is made is not known even though the initial temperature is known. Therefore a model is needed to predict the temperature of the heating element. The temperature rise of the heating element relative to the heat-sink is proportional to the input power

$$T = T_S + AP, \tag{2}$$

where T_s is the heat-sink temperature, P is the applied power for a fixed duration and A is a temperature model parameter that converts applied power to temperature. If the measurements are made for several on-times, a different value of A is used in Eq. (2) for each on-time. The measurement triplet is denoted as $\{R_i, T_{si}, P_i\}$, where the subscript i ranges from 1 to the number of measurements N. The relationship between the measurements is obtained from Eq. (2) as:

$$f(R_i) = T_{si} + AP_i. \tag{3}$$

Assuming the measurements are corrupted by Gaussian noise, the MLE for the function $f(\cdot)$ and A is obtained from Eq. (3) as:

$$\left[\hat{f}(\cdot), \hat{A}\right] = \underset{f(\cdot), A}{\arg\min} \sum_i \frac{1}{\sigma_i^2} \left(f(R_i) - T_{si} - AP_i\right)^2, \tag{4}$$

where σ_i is the standard deviation of the computed temperature difference arising from noise in the measurement triplet. In practice, the noise on the resistance measurements (σ_R) dominates and we can approximate σ_i as:

$$\sigma_i = \frac{df(R)}{dR}\sigma_R. \tag{5}$$

Substituting Eq. (5) into Eq. (4), we obtain:

$$\left[\hat{f}(\cdot), \hat{A}\right] = \underset{f(\cdot), A}{\arg\min} \sum_i \frac{1}{\left(df(R_i)/dR\right)^2} \left(f(R_i) - T_{si} - AP_i\right)^2. \tag{6}$$

We formulate non-parametric models for $f(\cdot)$ in the follow-ing sections to facilitate the optimization problem posed by Eqs. (4) and (6).

Polynomial Approximation for f(·)

A p[th] order polynomial representation for $f(\cdot)$ is given as:

$$f(R) = x_p R^p + x_{p-1} R^{p-1} + \ldots + x_0, \tag{7}$$

where x_j, $j = 0,\ldots p$, are the polynomial coefficients. We construct the following matrices and vector from the N measurements and the p+1 unknown polynomial coefficients:

$$\mathbf{R} = \begin{bmatrix} R_1^p & \cdots & 1 \\ \vdots & & \vdots \\ R_N^p & \cdots & 1 \end{bmatrix}, \mathbf{T}_s = \begin{bmatrix} T_{s1} \\ \vdots \\ T_{sN} \end{bmatrix}, \mathbf{P} = \begin{bmatrix} P_1 \\ \vdots \\ P_N \end{bmatrix}, \mathbf{x} = \begin{bmatrix} x_p \\ \vdots \\ x_0 \end{bmatrix}. \tag{8}$$

The solution to Eq. (4) is given as:

$$\begin{bmatrix} \hat{\mathbf{x}} \\ \hat{A} \end{bmatrix} = \left(\mathbf{D}^T \mathbf{W} \mathbf{D}\right)^{-1} \mathbf{D}^T \mathbf{W} \mathbf{T}_s, \tag{9}$$

where $\mathbf{W}$ is a diagonal weight matrix constructed as:

$$\mathbf{W} = \begin{bmatrix} 1/\sigma_1^2 & & \\ & \ddots & \\ & & 1/\sigma_N^2 \end{bmatrix}, \tag{10}$$

and $\mathbf{D}$ is defined as:

$$\mathbf{D} = [\mathbf{R} - \mathbf{P}] \tag{11}$$

The solution to Eq. (6) is more difficult since the weight matrix $\mathbf{W}$ depends on the derivative of the function we are trying to estimate. We solve this problem by estimating the parameters iteratively using Eq. (8). At each iteration, the weight matrix is recomputed using the derivative of the function estimated in the previous iteration in Eq. (5).

Piecewise Polynomial Approximation for f(·)

A global polynomial is not very effective in fitting local features of the function $f(\cdot)$. Increasing the order of the polynomial to improve the fit typically does not help and usually results in numerical instability. A better solution is to fit a number of lower order polynomials locally. Usually a piecewise linear approximation is good enough. The method of the previous section can be generalized to achieve this. Divide the domain of interest for the function $f(\cdot)$ into N_r regions. Let $r = I(R)$ denote the index of the region that R falls into. All the matrices and vectors defined in Eqs. (8) and (10) are now denoted with a subscript r. For example, the matrix $\mathbf{R}_r$ is constructed using only the resistance measurements for samples i such that $I(R_i) = r$, $\forall i$.

The solution to Eq. (4) is given as:

$$\begin{bmatrix} \hat{\mathbf{x}}_1 \\ \vdots \\ \hat{\mathbf{x}}_{N_r} \\ \hat{A} \end{bmatrix} = \left(\mathbf{D}^T \mathbf{W} \mathbf{D}\right)^{-1} \mathbf{D}^T \mathbf{W} \begin{bmatrix} \mathbf{T}_{s1} \\ \vdots \\ \mathbf{T}_{sN_r} \end{bmatrix}, \tag{12}$$

where

$$\mathbf{D} = \begin{bmatrix} \mathbf{R}_1 & & -\mathbf{P}_1 \\ & \ddots & \vdots \\ & \mathbf{R}_{N_r} & -\mathbf{P}_{N_r} \end{bmatrix} \text{ and } \mathbf{W} = \begin{bmatrix} \mathbf{W}_1 & & \\ & \ddots & \\ & & \mathbf{W}_{N_r} \end{bmatrix}. \tag{13}$$

The iterative solution to Eq. (6) may be performed in a fashion similar to that proposed in previous section.

The function estimated by this method will probably be discontinuous at the region boundaries because no continuity constraints have been imposed on the polynomial coefficients. This can be mitigated by overlapping the region boundaries. Furthermore, once A is estimated, the unknown temperature associated with each resistance measurement can be computed using Eq. (2). A spline may then be fitted to the resistance-temperature pairs to obtain the final continuous estimate of $f(\cdot)$.

Bias in the Temperature Scale Estimate

The joint estimation of $f(\cdot)$ and A tends to bias the temperature scale. The bias in the parameter estimates given by Eq. (4) is difficult to compute directly since the estimated function $f(\cdot)$ can take on an arbitrary shape. We simplify the problem by assuming that our estimates of $f(\cdot)$ and A differ from their true values by an unknown scalar s as follows

$$\hat{A} = sA$$
$$\hat{f}(R) = s\left(f(R) - \overline{T}_s\right) + \overline{T}_s, \text{ where } \overline{T}_s = \frac{1}{N}\sum_i T_{si}. \tag{14}$$

Then it can be shown that the expected value of s is given as

$$E[s] = \frac{1}{1+\text{SNR}^{-1}}, \text{ where SNR} \equiv \frac{1}{\text{N}}\sum_i \frac{\left(T_{si} - \overline{T}_s\right)^2}{\sigma_i^2}. \tag{15}$$

The bias in $\hat{A}$ is computed from Eq. (14) and (15) as

$$E\left[\hat{A}\right] - A = \frac{-A}{1+\text{SNR}}. \tag{16}$$

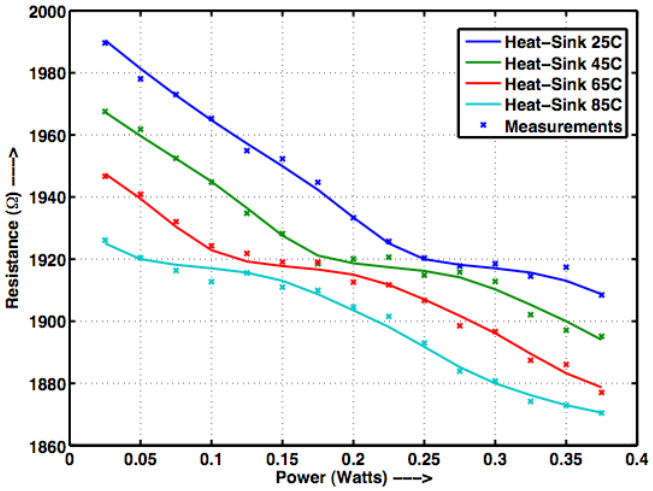

Figure 2. Synthetic Resistance measurements for various heat-sink temperatures and applied powers. Solid line shows true values and "crosses" show simulated measurements

Results

First consider a synthetic example in which we have access to the true model parameters so that we can assess the estimation accuracy of the different methods. Figure 2 shows the true values and simulated measurements of the resistances for 4 different heat-sink temperatures and 15 different power levels with A = 300°C/W and the ground truth $f(\cdot)$ shown in Fig. 3. Gaussian noise (σ_R = 2Ω) was added to the measurements. The average SNR for this data is 21. From Eq. (16), the expected value of A is 286 (a bias of -14°C/Watt) if the shape of the estimated function is the same as the ground truth.

Figure 3 compares the global and piecewise polynomial methods. In each case, the result of the second iteration is shown where the weight matrix has been recomputed using the derivative of the function estimated in the first iteration. We see that the global polynomial is not a very good fit even for higher orders (3rd order shown) and $\hat{A}$ =263°C/W is quite a bit lower than the true value. This was by design since the ground truth function had local features that are difficult to model with a global polynomial. On the other hand, the piecewise polynomial method reproduces the function accurately with $\hat{A}$ =294°C/W. The fit shown in Fig. 3 was obtained by dividing the resistance measurements into eight non-overlapping regions such that each region had the same number of samples. Each region used a first order polynomial. Choosing the regions in this manner has the advantage that we automatically get more definition for the unknown function in regions where there are more resistance measurements. The final estimate of $f(\cdot)$ is obtained by reconstructing the temperature using $\hat{A}$ in Eq. (2) and fitting a second order spline to the measurement samples.

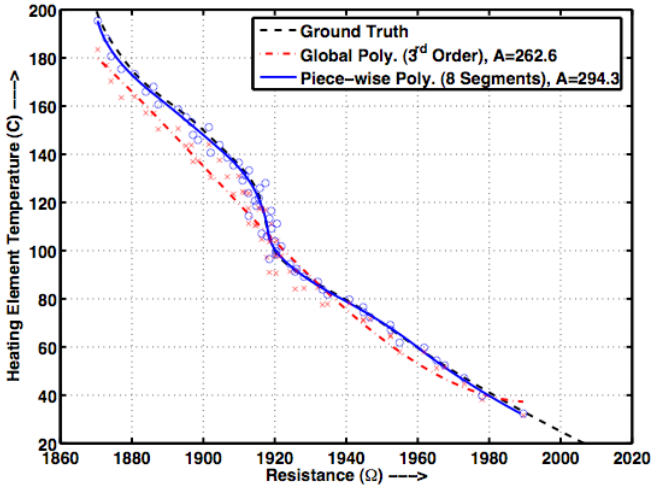

Figure 3. Estimated f(·) using global and piecewise polynomial methods. The reconstructed temperature for the resistance measurements are shown as "crosses" (global polynomial) and "circles" (piecewise polynomial)

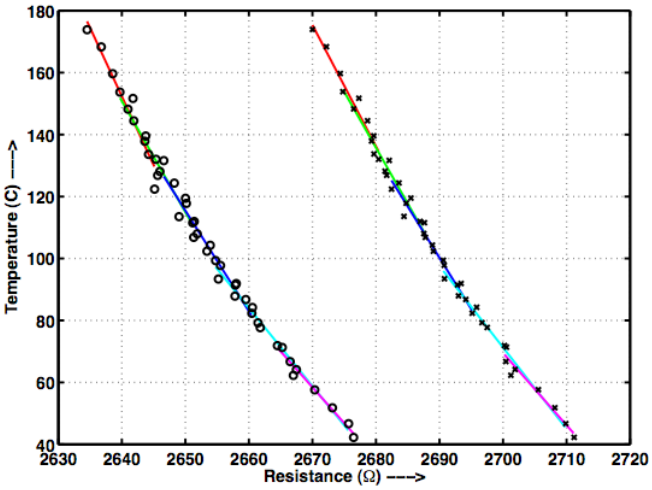

Figure 4. Piecewise linear fits to data collected on two elements of a Toshiba TPH separated by 64 elements. $\hat{A}$ = 310°C/W and 305°C/W for the two elements.

Figure 4 shows the piecewise linear fits to data collected from two heating elements of a Toshiba TPH. The elements were separated by 64 pixels spaced at 306dpi. Five different heat-sink temperatures (30°C, 50°C, 70°C, 90°C, 110°C) and nine different power levels ranging from 0.04W to 0.21W were used for the measurements. The fits were obtained using 4 regions with 75% overlap. The estimated values of A were 310°C/W and 305°C/W. It is not possible to assess the accuracy of these estimates since the ground truth is not available for this data. However, the fitting error yields an estimate for the temperature noise of 2.5°C, which is used to compute the SNR (130) and bias in $\hat{A}$ of approx. -1%.

Note that the temperature predicted for any resistance value is different for the two elements. However, if the material properties are similar for the two elements, the change in resistance for a unit change in temperature should be similar. Indeed, when the functions are plotted with respect to normalized resistances (not shown), there is good agreement between the two estimates and the differences are comparable to the noise.

Conclusion

We have shown that the simultaneous estimation of the temperature scale and resistance-temperature mapping is biased for the MLE. The bias may be reduced by lowering the measurement noise and/or increasing the range of the heat-sink temperatures for the resistance measurements. The piecewise linear method is best suited to reducing the model mismatch and bias since it can conform to any local feature of the resistance-temperature mapping. The model-based approach successfully estimates this mapping for temperatures much higher than the maximum heat-sink temperature used in the measurements.

A parametric model for the resistance change with temperature derived from the underlying physics of semiconductors[3] may be used for $f(\cdot)$. If the model accurately describes the heating element's material characteristics, it has the advantage of reducing the number of parameters that need to be estimated. Consequently, fewer measurements will be required to achieve the same accuracy as that of the non-parametric methods.

References

1. I. Fukushima, Thermal Head Apparatus, *U. S. Patent 5646672,* (1997)
2. S. S. Saquib and W. T. Vetterling, A Real-Time Multi-Resolution Algorithm for Correcting Distortions Produced by Thermal Printers, *Proc. of IS&T-SPIE Elec. Imaging Sym.,* Vol. 5674, pp 269-281, San Jose, CA (2005).
3. N. W. Ashcroft and N. D. Mermin, Solid State Physics, Saunders College Publishing, (1976)

Author Biography

Suhail S. Saquib received his B.Tech. degree in Electronics and Electrical Comm. Eng. from Indian Institute of Tech., Kharagpur, India, in 1991. He received his M.S. and Ph.D. degrees in EE from Purdue University in 1992 and 1997 respectively. During the summer of 1996, he worked at Los Alamos National Laboratories in the area of medical optical tomography. Since 1997 he has been with the Image Science Lab. at Polaroid Corporation. His work has focused on physical modeling of photographic systems and model-based computational algorithms for improving image quality.